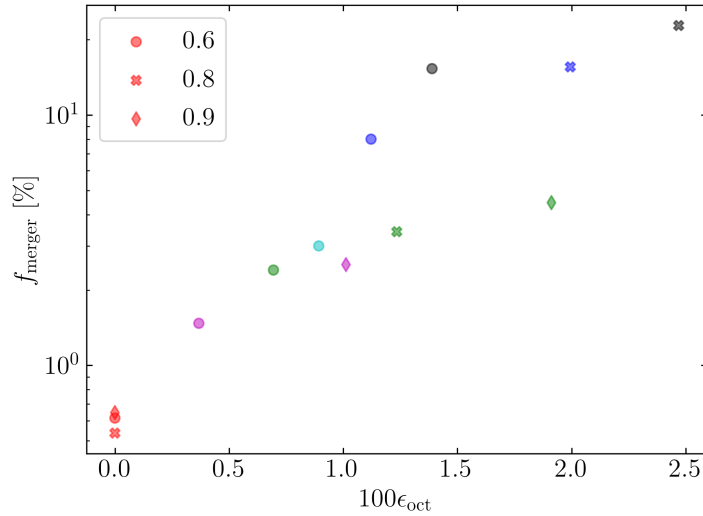


## 1 Executive Summary

- In the regime where  $e_{\text{lim}}$  is sufficient to induce one-shot mergers, the inclinations  $I_0$  where  $e_{\text{lim}}$  is attainable correspond very well with the regions where the octupole-induced merger probability is nonzero.
- Furthermore, there are regions where “octupole-enhanced” mergers occur. This is because octupole effects excite the suitably-averaged eccentricity enough that mergers occur within a Hubble time. This effect is much more substantial for smaller  $a$ , where one-shot mergers are difficult.
- For  $I_0$  sufficiently close to  $90^\circ$ , finite  $\eta$  suppresses octupole-LK excitation to  $e_{\text{lim}}$ .

## 2 Simulations



**Figure 1:** Total merger fractions. Different symbols denote different  $e_{\text{out}}$  (legend), and different colors denote different  $q \in [0.2, 0.3, 0.4, 0.5, 0.7, 1.0]$  (darker colors correspond to smaller  $q$ ). I will have  $q = 1.0, e_{\text{out}} = 0.9$  ready by tomorrow.

10 AU is hard to run, RAM intensive and takes many cycles to merger. I tried to run too dense of a grid of simulations and also had some RAM issues on accident, didn’t finish. But most of the behavior can be seen in the 100 AU simulations that I ran, which are much faster ( $t_{\text{LK}} \propto a^{3/2}$ ).

Tried to run wide range of simulations for  $\{q \in [0.2, 0.3, 0.5, 0.7, 1.0]\} \otimes \{e_{\text{out}} \in [0.6, 0.8, 0.9]\}$  while holding  $a_{\text{out,eff}} = 3600 \text{ AU}$  ( $e_{\text{out}} = 0.6, a_{\text{out}} = 4500 \text{ AU}$ ) constant. The other parameters are, as before:

$$m_{12} = 50M_{\odot}, \quad m_3 = 30M_{\odot}, \quad a_{1,0} = 100 \text{ AU} \quad e_{1,0} = 10^{-3}.$$

Of the 18 parameter regimes targeted, 13 have complete data. The current merger fraction plot is in Fig. 1.

However, I do reproduce the “gap” that Bin saw. A characteristic plots are shown in Figs. 2–5.

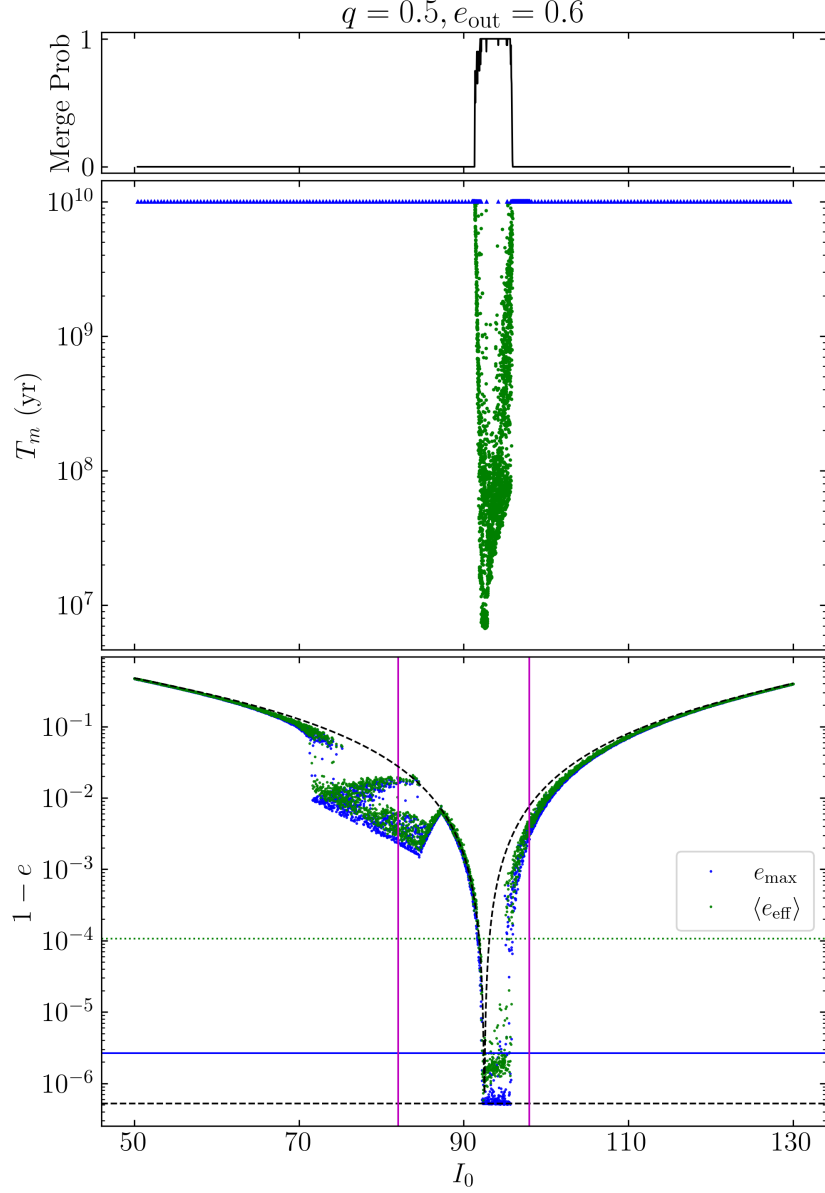


**Figure 2:** Example 1. Top panel is merger probability, middle panel is merger times (green dots are mergers, blue triangles are non-merging systems), and the bottom panel is the plot of  $1 - e$  without GW run over  $500t_{\text{LK}}$ . On the bottom panel, the black dashed curve represents the quadrupole  $e_{\max}$  values [analytic, LL18 Eq. (42)], the blue dots represent the  $e_{\max}$  over the GW-less run, and the green dots represent the average  $e_{\text{eff}}$  [Eq. (9)] over the same interval; the horizontal lines correspond to  $e_{\text{lim}}$  (black), the one-shot merger eccentricity  $e_{\text{os}}$  (blue), the necessary effective eccentricity to merge  $e_{\text{eff,c}}$  (green); and the pink vertical lines represent  $I_{\text{lim}}$  given by MLL16 for reference. In broad summary, systems with  $e_{\max}$  below the blue line are expected to merge, as are systems with  $\langle e_{\text{eff}} \rangle$  below the green line.

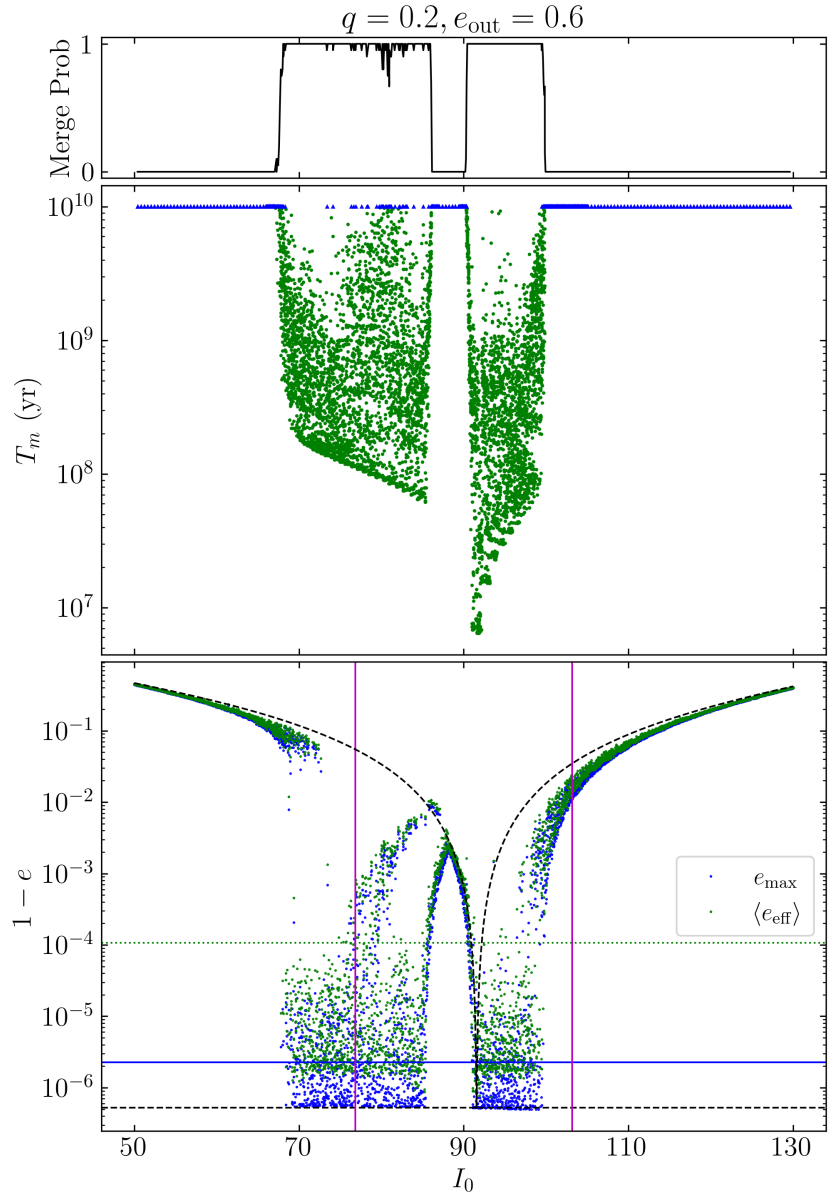


**Figure 3:** Example 2

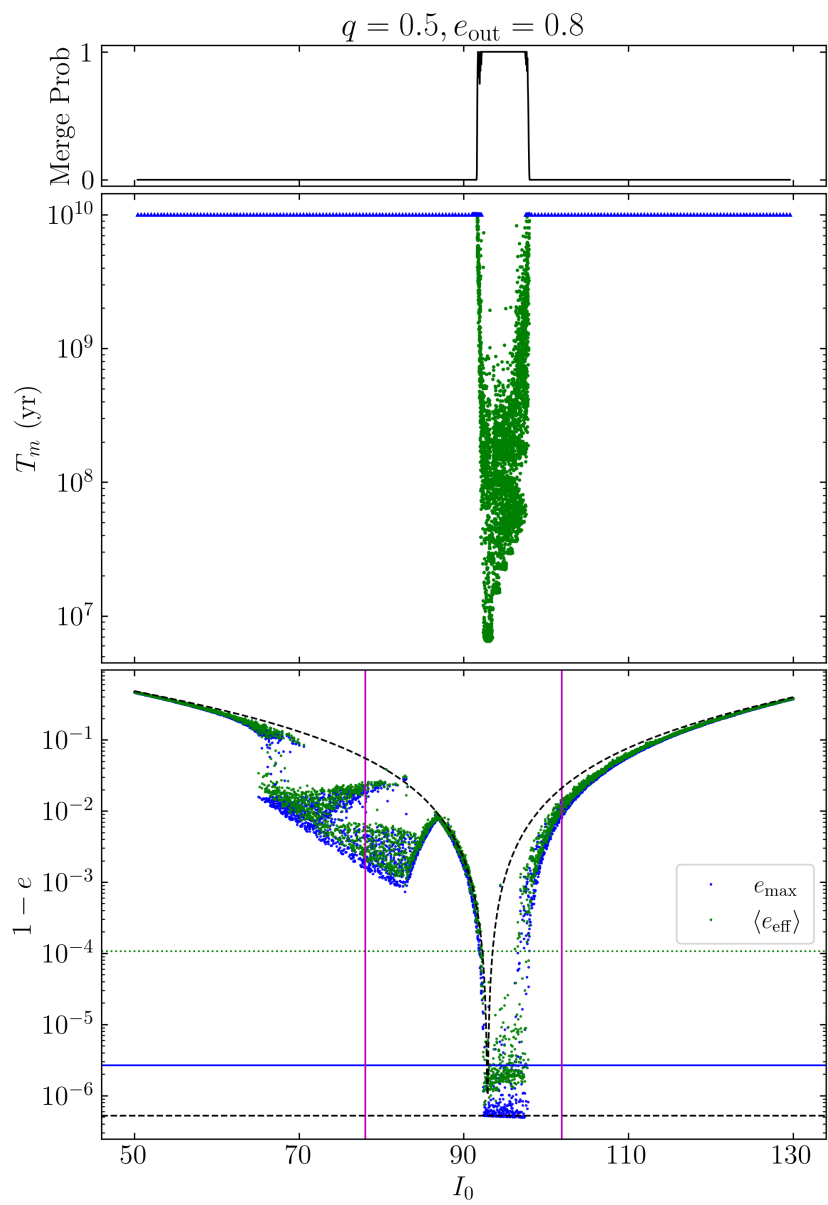


**Figure 4:** Example 3

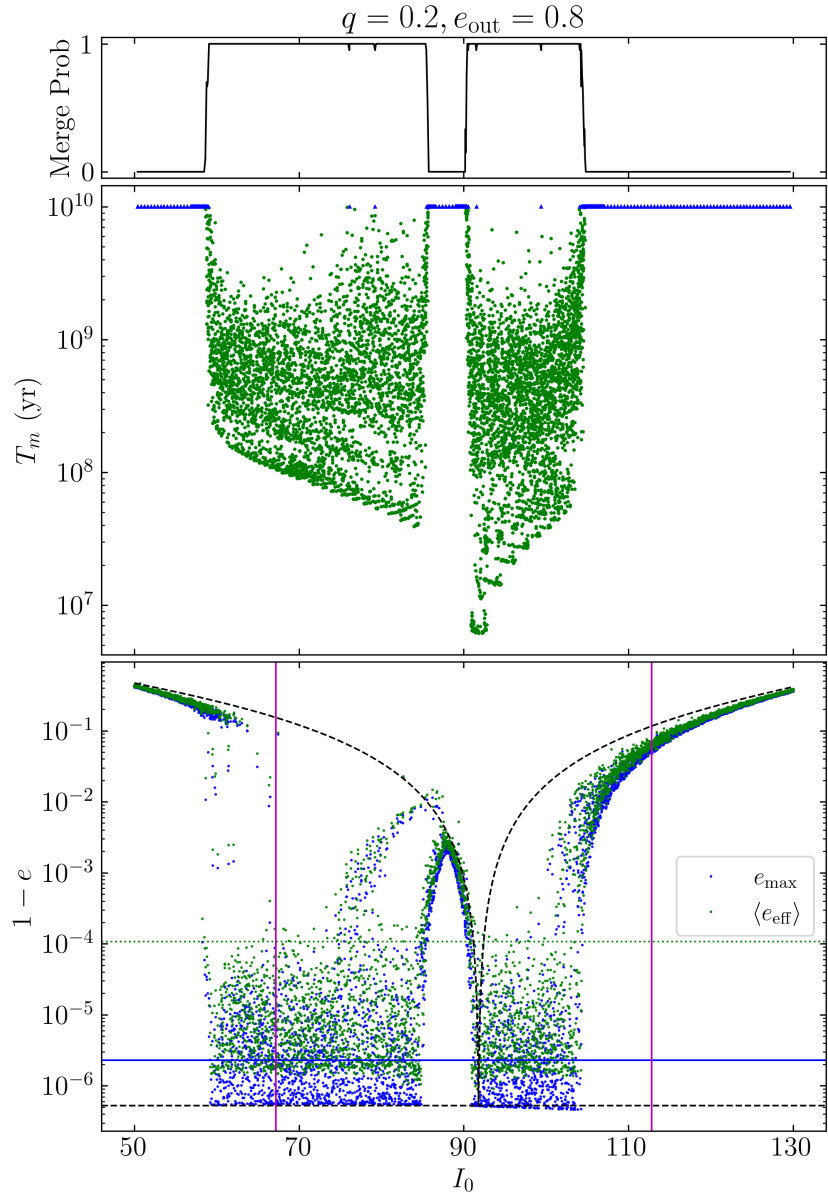


**Figure 5:** Example 4

### 3 Theory

#### 3.1 One-Shot Merger Eccentricity

We seek a critical  $e_{\text{os}}$  for which the system can merge in “one-shot”, i.e. in one LK cycle. This can be computed:

$$\frac{d \ln a}{dt} = -\frac{64}{5j^7(e)} \left( 1 + \frac{73}{24}e^2 + \frac{37}{96}e^4 \right) \frac{G^3 \mu m_{12}^2}{c^5 a^4}, \quad (1)$$

$$\sim -j(e_{\text{max}}) \frac{64}{5j^7(e_{\text{max}})} (4) \frac{G^3 \mu m_{12}^2}{c^5 a^4}, \quad (2)$$

$$j^6(e_{\text{os}}) \equiv j_{\text{os}} = \frac{256}{5} \frac{G^3 \mu m_{12}^2}{c^5 a^4} \frac{1}{n} \frac{m_{12}}{m_3} \left( \frac{a_{\text{out,eff}}}{a} \right)^3, \quad (3)$$

$$= \frac{256}{5} \frac{G^3 \mu m_{12}^3}{m_3 c^5 a^4 n} \left( \frac{a_{\text{out,eff}}}{a} \right)^3. \quad (4)$$

Thus, when systems satisfy  $e_{\text{lim}} \gtrsim e_{\text{os}}$ , all orbit flips will lead to mergers. We can approximately solve to find (to be checked)

$$j_{\text{lim}} \approx \frac{8\epsilon_{\text{GR}}}{9 + 3\eta^2/4}, \quad (5)$$

$$\left( \frac{a}{a_{\text{out,eff}}} \right) \gtrsim 0.0118 \left( \frac{a_{\text{out,eff}}}{3600 \text{ AU}} \right)^{-7/37} \left( \frac{m_{12}}{50 M_{\odot}} \right)^{17/37} \left( \frac{30 M_{\odot}}{m_3} \right)^{10/37} \left( \frac{q/(1+q)^2}{1/4} \right)^{-2/37}. \quad (6)$$

This is the regime in which ELK-induced mergers is easiest to understand.

#### 3.2 Effective Merging Eccentricity

Some systems can merge even without undergoing orbit flips. These correspond to the probabilistic regions. We define an “effective” eccentricity, over the GW-less simulations, such that the total GW emission is comparable:

$$\left\langle \frac{d \ln a}{dt} \right\rangle = - \left\langle \frac{a}{t_{\text{GW}}} \right\rangle, \quad (7)$$

$$\approx -\frac{a}{t_{\text{GW},0}} \left\langle \frac{1 + 73e_{\text{max}}^2/24 + 37e_{\text{max}}^4/96}{j^6(e_{\text{max}})} \right\rangle, \quad (8)$$

$$\equiv -\frac{a}{t_{\text{GW},0}} \underbrace{\left( \frac{1 + 73e_{\text{eff}}^2/24 + 37e_{\text{eff}}^4/96}{j^6(e_{\text{eff}})} \right)}_{f(e_{\text{eff}})} \approx \frac{-4a}{t_{\text{GW},0} j^6(e_{\text{eff}})} \quad (9)$$

where the average is taken over many LK cycles, and  $t_{\text{GW},0}$  denotes the  $e = 0$  evaluation.

We can then ask what level of  $e_{\text{eff}}$  is required to induce merger within a Hubble time  $t_{\text{Hubb}}$ . This can also be estimated

$$\frac{t_{\text{GW},0}}{t_{\text{Hubb}}} \frac{1}{f(e_{\text{eff}})} \lesssim 1, \quad (10)$$

$$\left( \frac{4t_{\text{Hubb}}}{t_{\text{GW},0}} \right)^{1/6} \gtrsim j(e_{\text{eff}}), \quad (11)$$

$$0.01461 \left( \frac{100 \text{ AU}}{a} \right)^{2/3} \left( \frac{1/4}{q(1+q)^2} \right)^{1/6} \gtrsim j(e_{\text{eff}}), \quad (12)$$

$$1 - e_{\text{eff}} \lesssim 1.068 \times 10^{-4}. \quad (13)$$

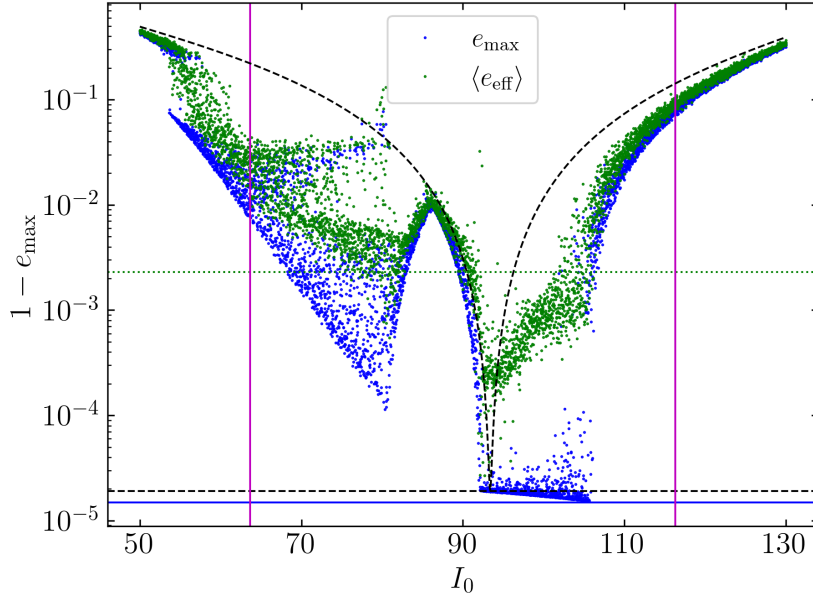


**Figure 6:**  $e_{\max}$  distribution for Bin’s gapped case last week. Note that  $e_{\lim} \approx e_{\text{os}}$  for this parameter regime.

We can see that the probabilistic regime in the earlier figures is where  $e_{\text{eff}}$  spans a few orders of magnitude. This suggests that  $e_{\text{eff}}$  stochastically attains these large values over timescales  $\gg 500t_{\text{LK}}$  (i.e. over time, some fraction of systems will enter a very high maximum-eccentricity state).

### 3.3 Origin of the Gap

We have already reproduced the gap in our simulations. For reference, we can also look at  $e_{\max}$  distribution for Bin’s case from last week  $a_{\text{out}} = 700$ ,  $e_{\text{out}} = 0.9$ ,  $a_{\text{in}} = 10$  AU, and  $q = 0.4$  in Fig. 6 (NB: I messed up and used  $m_{12} = 50M_{\odot}$  while Bin used  $m_{12} = 60M_{\odot}$ ).

The origin of the gap is because  $e_{\max}$  oscillations are suppressed near  $I = 90^\circ$ . I think this happens because Katz et. al. 2011 show that ELK oscillations happen due to a feedback between  $j_z = j \cos I$  (conserved to quadrupole order in the test mass limit) and  $\Omega_e$  the co-longitude (? azimuthal angle relative to  $\hat{\mathbf{z}}$ ) of the inner eccentricity vector. However, when  $\eta > 0$ , we know that the conserved quantity is

$$K \equiv 2j \cos I + \eta j^2. \quad (14)$$

This suggests that when  $j \cos I \lesssim \eta$ , that  $\eta$  suppresses the feedback and the ELK oscillations. I think this is the right mechanism, but I don’t have the analytical solution.